HHS Public Access

Author manuscript

Mod Pathol. Author manuscript; available in PMC 2021 January 02.

Published in final edited form as:

Mod Pathol. 2020 December ; 33(12): 2449–2457. doi:10.1038/s41379-020-0605-1.

Detection and assessment of capsular invasion, vascular invasion and lymph node metastasis volume in thyroid carcinoma using microCT scanning of paraffin tissue blocks (3D whole block imaging): a proof of concept

Bin Xu, **Alexei Teplov**, **Kareem Ibrahim**, **Takashi Inoue**, **Ben Stueben**, **Nora Katabi**, **Meera Hameed**, **Yukako Yagi**, **Ronald Ghossein**

Department of pathology, Memorial Sloan Kettering Cancer Center

Abstract

In the modern era, detailed pathologic characteristics of a thyroid tumor are crucial to achieve accurate diagnosis and guide treatment. The presence of capsular invasion (CI) is diagnostic for carcinoma, whereas vascular invasion (VI) and nodal metastasis (NM) are included in risk stratification. However, the very definition of CI and VI is surrounded by controversies and an accurate assessment of NM is lacking. Whole Block Imaging (WBI) by microCT is a new imaging modality to create 3D reconstruction of whole tissue block with microscopic level resolution without the need for tissue sectioning. In this study, we aimed to define CI, VI, and NM volume using WBI by microCT. Twenty-eight paraffin blocks (PBs) from 26 thyroid tumors were scanned. Ten PBs contained CI, whereas 7 had VI. 3D microCT images were compared with whole slide images (WSI) of corresponding H&E slides. In 2 cases with VI and/or CI, WSI of serial H&E slides were obtained and underwent 3D-reconstruction to be compared with the WBI. Satellite tumor nodules beyond tumor capsule were shown to be CI by demonstrating the point of penetration using microCT and 3D reconstruction. Additional foci of CI were detected using microCT. VI was seen using microCT. Fibrin associated with tumor thrombus was not always present on serially sectioned H&E slides. WBI by microCT scanner was able to assess the volume of NM. In conclusion, WBI is able to detect CI, VI, and assess the volume of NM in thyroid carcinoma without tissue sectioning. It is the ultimate method for the complete sampling of the tumor capsule. It has the potential to increase the detection rate of CI, better define criteria for CI and VI and provide an accurate assessment of the volume of nodal disease. This technology may impact the future practice of surgical pathology.

Keywords

whole block imaging; microCT; thyroid carcinoma; capsular invasion; vascular invasion

Corresponding authors: Ronald Ghossein, MD, Department of Pathology, Memorial Sloan-Kettering Cancer Center, 1275 York Avenue, New York, New York, 10065, ghosseir@mskcc.org; Yukako Yagi, PhD, Department of Pathology, Memorial Sloan-Kettering Cancer Center, 1275 York Avenue, New York, New York, 10065, yagiy@mskcc.org.

Disclosure Statement: No competing financial interests exist for all contributory authors. No competing financial interests exist for all contributory authors.

Introduction

The accurate diagnosis of a well-differentiated follicular cell-derived thyroid neoplasm is based on a combination of multiple histologic features, including architectural pattern, nuclear features, encapsulation, capsular invasion (CI) and vascular invasion (VI) (1, 2). In addition, clinical management guidelines, e.g. the American Thyroid Association (ATA) and the National Comprehensive Cancer Network (NCCN) guidelines, include risk stratification models that encompass many pathologic parameters, e.g. extent of VI, number and size of nodal metastasis, gross and microscopic extrathyroidal extension, histotypes and variants of carcinoma (3, 4). All of these pathologic parameters are defined primarily based on histologic features detected on hematoxylin and eosin (H&E) stained slides.

In recent years, new imaging modalities have emerged in the field of diagnostic pathology. Multiple large-scale studies have shown that whole slide imaging (WSI) has similar imaging equivalency and efficiency as conventional microscopic examination of H&E glass slides, which led to the Food and Drug Administration (FDA, USA) approval of WSI for clinical use (5, 6). Additionally, three-dimensional (3D) imaging and reconstruction of serial WSIs as well as 3D whole block imaging (WBI) using micro-resolution computed tomography (microCT), have been developed to provide additional accuracy in assessing pathology parameters, e.g. tumor size and margin status (7-10).

MicroCT is a novel *in vitro* tomographic method allowing examination of fresh tissue or paraffin blocks. Similar to the CT scan used in radiology, the images obtained are the result of difference in X-Rays absorption but with a spatial resolution up to the level of 1 micron (9-11). Compared with serial H&E sectioning with or without subsequent 3D reconstruction, microCT has the advantages of non-invasiveness and preservation of tissue within the paraffin blocks (9-11).

In this study, we aimed to explore the utility of WBI using microCT in thyroid tumor pathology, in particular the definition of various crucial pathologic parameters, using a combination of conventional techniques (e.g. H&E slides and serial sections) and novel imaging modalities (e.g. WSI with 3D reconstruction and WBI using microCT).

Material and Methods

Case selection

The study was approved by the Institutional Review Board (IRB) of Memorial Sloan-Kettering Cancer Center. A total of 28 paraffin blocks from 26 thyroid tumors were included in this study. The pathologic diagnosis was rendered as part of the routine clinical pathology practice after reviewing all the H&E slides by endocrine pathologists. Based on the gross examination and/or slides review, an average of 3 blocks and a median of 2.6 blocks per cm of tumor were submitted for microscopic examination and their corresponding slides reviewed. The capsule of all primary tumors was entirely submitted for microscopic examination. One or two H&E slides per tumor showing key features of interests (e.g. CI or VI) and their matched paraffin blocks were selected by two endocrine pathologists (BX and

RG), and subsequently subjected to WSI of the H&Es and microCT WBI of the blocks. The H&E was sectioned from the surface of the paraffin blocks without further trimming or additional sectioning.

The tumor types included were papillary thyroid carcinoma (PTC, n=11), Hurthle cell carcinoma (HCC, n=7), noninvasive follicular thyroid neoplasm with papillary-like nuclear features (NIFTP, n=7), and follicular thyroid carcinoma (FTC, two blocks from one tumor). Among the 11 PTCs included, nine were classic variant (including eight primary thyroid tumors, and two blocks from one patient with nodal metastases), one was an encapsulated follicular variant with invasion, and one was a solid variant. None of the blocks included demonstrated lymphatic invasion on the initial H&E sections.

WBI using MicroCT

The workflow is depicted in Figure 1. The 28 paraffin blocks were scanned with a microCT. The micro-CT imaging system consists of a custom built micro-CT scanner (Nikon Metrology NV, Leuven, Belgium) and data reconstruction software CT Agent Medical Alpha version XT 5.1.4.2 MedX1 (Nikon Metrology NV). Scanned image data is stored in a data storage server in our institutions data center. Scanned image slices were reconstructed using modified Feldkamp filtered back projection algorithms with CDPro3D (Nikon Metrology, Belgium) with appropriate parameter per image type and resolution. The re-constructed imaging data were visualized and analyzed by using commercially available software for 3D imaging such as VG Studio M2.2.6(Volume Graphics GmbH, Heidelberg, Germany) and Dragonfly 3.1(Object Research Systems, Montreal, Quebec, Canada). These applications allow construction and analysis of 3D data, separation and extraction of object of interests, for data to be measured, quantified and filtered in all dimensions. The greyscale microCT images obtained were then subsequently digitally colorized to simulate a H&E image (H&E like appearance).

WSI, serial sectioning, and 3D reconstruction

An initial H&E slide per paraffin block was digitally scanned to WSI using a Nanozoomer2.0 HT (Hamamatsu Photonics, Hamamatsu, Japan) at 20X magnification (0.46 micron/pixel). 100 Serial 4-micron sections were obtained with AS-410 Automated Tissue Sectioning System (Dainippon Seiki, Kyoto, Japan) in two cases, a HCC with one focus of CI and one focus of VI, and a HCC with two foci of VI. The serial WSIs were subsequently subjected to 3D reconstruction using Voloom (version 2.8.3, microDimensions GmbH, München, Germany).

Images from the WSI and WBI were compared for various histologic features, including architecture features (e.g. papillae vs. follicle), the presence and extent (number of foci) of CI and VI to determine the utility of WBI and to define crucial parameters in thyroid tumors.

Estimation of volume of lymph node metastasis

Two paraffin blocks from two lymph nodes with metastatic PTC were included in this study. Each paraffin block contained one bisected lymph node. The outline of the metastatic foci was annotated on WSI of the H&E slide and 3D microCT images. Three measurements were

taken for each nodal metastasis: 1) the maximal linear dimension (length) of the metastatic focus on WSI, 2) the total area (including both halves of the bisected lymph nodes) of metastases on WSI, and 3) the total volume of metastasis measured in 3D WBI using microCT.

Results

Capsular invasion

WBI was performed on 10 blocks containing CI, including three PTCs classic type, one PTC encapsulated follicular variant, four HCCs, and two blocks from one FTC. A block of NIFTP with incomplete penetration of the tumor capsule was also included. The remaining 15 blocks of primary tumor did not show CI on WSI and WBI.

Characteristics of CI observed in WSI and WBI are summarized in Table 1 and Figure 2. CI could be easily identified in microCT images at a resolution of pixel size 10.6 – 16.9 um and pixel size 5.1-6.3 um.

Among the 10 blocks studied, four cases (40%) with satellite nodules detected on initial H&E WSI showed point of penetration on WBI, and one case (10%) with the initial H&E showing a CI with point of entry became a satellite nodule on WBI. Serial H&E slides and 3D reconstruction of one paraffin block of HCC further confirmed such findings detected by WBI (Supplementary material, video 1: 3D-reconstruction of serial WSI, video 2: WBI by microCT).

One block per tumor was subjected to microCT WBI. Among the 10 blocks scanned, two (20%) showed additional foci of CI in WBI compared with one H&E slide.

We also included a single NIFTP case with incomplete penetration of the capsule on the initial H&E. The focus remained as incomplete penetration on WBI (Supplementary figure 1). The diagnosis was NIFTP before and after WBI.

Vascular invasion

WBI using microCT was obtained in seven blocks showing VI of venous caliber vessels within the tumor capsule on the initial H&E sections, including five HCCs, a PTC encapsulated solid variant, and a PTC encapsulated classic variant with predominant follicular pattern. Invasion of small capillary-sized vessels (lymphatic or blood vessel) was not evaluated in this study as the current resolution of WBI did not allow identification and visualization of these vessels. Additionally, serial H&E sections and subsequent 3D-reconstruction were performed on 2 blocks of HCCs with VI. The remaining 19 blocks of primary tumors did not show VI on WSI and WBI.

VI could be appreciated in WBI. Additionally, WBI may show point of entry, i.e. the site where the tumor penetrates into the vascular lumen (Figures 3 and 4). However, the resolution of microCT at present is insufficient for diagnosing VI based on WBI alone. Elements included in the current diagnostic criteria of VI, e.g. the identification of endothelial cells lining the vascular space and tumor embolus and/or fibrin microthrombus,

cannot be appreciated in the microCT images. Similarly, given the insufficient resolution, WBI using microCT cannot provide an accurate evaluation of the extent of VI.

Serial H&E sections and WSI from the two blocks of HCC with VI showed that fibrin associated with tumor thrombi was not always present on every level examined from a single focus of VI (Figure 4). In other words, one focus of VI had fibrin associated with the tumor thrombus in certain but not all histologic levels when serial sections were examined.

Evaluation of lymph node metastasis

WBI using microCT was performed on two paraffin blocks from one patient with metastatic PTC to lymph nodes to assess the utility of WSI and WBI in evaluating nodal metastasis. Each block contained a bisected node with metastatic PTC. The results are shown in Table 2 and Figure 5. The metastatic foci were readily identified in the microCT images. Although the maximal length of the two nodal metastases only differed by 2.367 folds, the total area of metastasis obtained using 2D WSI and 3D WBI changed by 8.465-folds and 13.125-folds. It therefore appears that metastatic tumor volume obtained using 3D WBI technique provided the most accurate measure of the difference in tumor burden between the two different nodes.

The utility of WBI to assess architecture in thyroid neoplasms

Aiming to study if WBI using microCT had sufficient resolution to distinguish papillae, pseudopapillae, and follicles, we performed microCT scanning on eight blocks of primary classic variant with various percentage of papillae, and seven blocks of NIFTPs defined using the original consensus criteria (12). Among the seven NIFTPs included, one contained <1% well-formed papillae, three showed pseudopapillae (defined as papillary projections lacking fibrovascular cores), and the remaining three were composed entirely of follicles on the initial H&E sections. At its highest resolution, microCT WBI could show architectural patterns (e.g. papillae and follicles) (Figure 6). However, histologic details, e.g. fibrovascular core, were not readily identified in WBI.

Discussion

Capsular invasion

In encapsulated thyroid neoplasms, the presence of invasion, being CI or VI, is the most important criterion to separate benign neoplasms from malignancy (2, 13, 14). Currently, CI is defined as complete penetration of tumor capsule by neoplastic cells in major guidelines, e.g. World Health Organization (WHO) classification (2), College of American Pathologist (CAP) checklist (13) and International Collaboration on Cancer Reporting (ICCR) dataset (14). In certain cases, a neocapsule, defined as a fibrotic stromal reaction forming a secondary limiting fibrous band at the site of CI, may be present (2). However, there is controversy on whether a satellite nodule, defined as a nodule with similar architectural and cytologic features to the main tumor, lying outside of the tumor capsule represents CI (14). For some authors (15), one should demonstrate the point of penetration in order for the satellite nodule to qualify as CI while for others this is not necessary (16). As important as the definition of capsular invasion is the issue of adequate sampling of the capsule in a

thyroid neoplasm. The microscopic examination of the entire capsule of a thyroid tumor is key to confirm or exclude a diagnosis of malignancy and is required for the diagnosis of NIFTP (12).

In this study, we have demonstrated that WBI using microCT is a rapid and noninvasive ancillary tool to investigate CI in thyroid neoplasms. It detects CI with an accuracy parallel to traditional H&E slides. Additionally, it allows detection of additional foci of CI within the paraffin blocks without the physical sectioning of the tissue (virtual recuts) (Figure 1). It may be the ultimate sampling method in encapsulated thyroid neoplasms since the whole capsule is examined in 3D. To achieve the same degree of sampling in just one plane using traditional H&E, one would have to cut at least 750 tissue sections from the 3 mm thick tissue usually present in a paraffin block. Lastly, we show that a satellite nodule is a form of CI and should be included as a criterion for invasion in thyroid neoplasms.

Vascular invasion

Currently, major guidelines have different definitions of VI in thyroid carcinoma: while the ICCR dataset (14) and the WHO classification of endocrine tumors (2) define VI as tumor thrombus present in an intracapsular vessel attached to its wall, covered by endothelial cells or associated with fibrin; the college of American pathologists (CAP) checklist only considers “invasion of tumor through a vessel wall accompanied by fibrin thrombus” as “unequivocal and meaningful vascular invasion” (13). Such definition renders the presence of fibrin thrombus a mandatory element to definite VI. As a result, endothelialized tumor embolus without fibrin would not be counted as significant VI.

This rigorous criterion of VI was included in the CAP cancer checklist based on the findings of a single study (17). Using associated fibrin thrombus as the new definition for VI, the rate of VI decreased to 3% and the frequency of distant metastasis from tumors with a single focus of VI was 35% (17). These authors hypothesized that the presence of fibrin thrombus was indicative of activation of coagulative cascade by tumor cells and a manifestation of true VI.

Herein, we serially sectioned two cases of HCC with VI defined using ICCR and WHO criteria. We have demonstrated that a single focus of VI may be associated with fibrin thrombi on certain histologic levels but not others. Clearly, fibrin thrombus, when formed adjacent to a tumor embolus, is not present throughout the entire focus of VI.

It is our routine practice in pathology to sample a single 4-micron H&E slide from a 3-mm thickness paraffin block with a sampling rate of approximately 1:750 of the tissue volume. Given this sampling rate, it would not be uncommon for the fibrin associated with a tumor thrombus to be missed by one representative H&E slide per paraffin block. Therefore, mandating visualization of fibrin to define VI will result in under diagnosis of VI. The findings of the present study therefore lend support to the criteria defined by ICCR dataset and the WHO classification to evaluate VI in thyroid tumors.

Additionally, we compared the performance of WSI of H&E and WBI using microCT in detecting VI. Although the WSI and WBI images correlated well with the focus of VI, WBI

at its current resolution cannot serve as a stand-alone tool for VI as crucial details (such as endothelial cells) are not readily visible in microCT images. In addition, microCT at this stage of its development cannot distinguish between blood vessel and lymphatic invasion. The latter distinction is now required by expert endocrine pathologists since blood vessel invasion indicates potential distant metastasis while lymphatic invasion does not. (13). Because the current resolution of WBI does not allow differentiation between various types of cells, it cannot be used to distinguish tumor thrombi in vascular spaces from other intravascular space-occupying lesions, e.g. intravascular papillary endothelial hyperplasia ("Masson's lesion") (18, 19). H&E slide remains the gold-standard method to evaluate VI.

Assessment of architectural pattern using WBI

Papillary thyroid carcinoma, the most common type of thyroid carcinomas, can be further divided into multiple subtypes (or variants) in part based on its architectural features (2). The two most common variants are the classic and follicular variants (20). The classic (or usual) type of PTC contains well-formed papillae with fibrovascular core, whereas the follicular variant is composed exclusively of follicles.

In 2016, NIFTP has been proposed by a panel of expert thyroid pathologists as the new nomenclature for noninvasive follicular-patterned lesions with nuclear atypia (12). The major aim of this nomenclature change is to eliminate "carcinoma" from the diagnosis given the extremely indolent clinical behavior with (near) zero risk of metastases and recurrence (12). The original diagnostic criteria allow ≤1% of papillae. However, soon after, the consensus group has modified the criteria of NIFTP to absence of any true papillae with fibrovascular core (21, 22). Therefore, it is important for a pathologist to distinguish true papillae from pseudopapillae (i.e. papillary structures lacking a fibrovascular core) or artifactually ruptured follicular septae simulating papillae as well as to identify a small percentage of papillae in thyroid lesions.

In this study, we analyzed the effectiveness of WBI as an alternative noninvasive method to evaluate architecture in thyroid lesions. Unfortunately, although one can distinguish papillae and follicles on WBI images, microCT at its current resolution is not sufficient to identify fibrovascular core and to distinguish pseudopapillae from true papillae. Future advances in the microCT technology with improved resolution are required in order to apply this imaging modality to the evaluation of architecture in thyroid pathology.

Evaluation of nodal metastasis

The size of nodal metastasis is one parameter included in the risk stratification of ATA and NCCN guidelines (3, 4). Small volume of nodal metastases, defined as 5 or less positive lymph nodes with the largest metastatic focus measuring less than 0.2 cm in greatest dimension is considered as an ATA low risk lesion, which does not mandate a completion thyroidectomy and/or post-operative radioactive iodine. In contrast, a metastatic focus of 3 cm or more in greatest linear dimension is considered as an ATA high risk lesion which requires total thyroidectomy and post-operative radioactive iodine ablation (3). In a recent meta-analysis, Randolph et al. have shown that microscopic pathologic N1 disease, defined as five or fewer positive lymph nodes and none equal or more than 1 cm in size, does not

significantly impact survival of patients with PTC (23). Therefore, it is crucial for pathologists to provide an accurate measurement of nodal metastases at the time of initial resection. How to measure these positive nodes can be challenging. In a retrospective study of 246 PTC with nodal metastasis conducted in our institution, the presence of a large sized positive node correlated with shorter recurrence free survival while the size of the largest metastatic tumor focus was unable to predict outcome in patients (24). We postulated that this lack of correlation could be due to the difficulty in assessing metastatic tumor burden in a lymph node using a unidimensional measurement of the largest metastatic focus. The latter measure may not be an accurate representation of metastatic tumor volume (24).

In this study, we attempted to solve this issue by analyzing the feasibility of WSI of H&E and WBI using microCT in providing an accurate measurement of nodal metastases. Two different nodes containing different sized metastatic papillary thyroid carcinoma foci were subjected to microCT. Although the maximal length of the two nodal metastases studied only differed by 2.367 folds, the volume of the metastatic foci calculated using 3D WBI varied by 13.125-folds. Clearly, the traditional unidimensional measure of a metastatic focus can lead to an erroneous assessment of the metastatic burden. This finding could explain the discrepant results obtained in our previous study when comparing the prognostic value of lymph node size vs metastatic focus dimension in PTC (24). Our data suggests that volume of nodal metastasis is the most accurate measurement compared with the 2D area and the linear measurements. Combining accuracy and noninvasiveness, 3D microCT is a novel rapid technique that may be utilized in thyroid pathology to assess the disease load in neck lymph nodes. Future large-scale studies are needed to clarify the prognostic values of metastatic volume obtained through 3D microCT WBI compared with the traditional linear measurement of the metastatic focus. If volume of nodal metastasis calculated by microCT is shown to have additive prognostic value in large studies on PTC, it can better stratify patients for therapy. This technique could be used in calculating nodal tumor burden in malignancies other than thyroid such as breast carcinomas.

In conclusion, WBI by microCT scanner is a novel noninvasive imaging technique with high resolution that allows the detection of capsular invasion in encapsulated thyroid carcinoma. It can detect additional foci of CI missed by the initial H&E without tissue exhaustion acting like virtual recuts. Although the resolution of WBI is not sufficient at the present time to detect vascular invasion and fine architecture details in thyroid carcinomas, it can shed light on the microanatomy of VI. Importantly, it can accurately evaluate the volume of the nodal metastasis in thyroid carcinoma potentially introducing a novel and better measure of nodal disease burden. If the latter parameter is shown to be superior to traditional histologic measurement of metastatic foci in large studies, it can help better stratify thyroid carcinoma patients. This new measure of metastatic disease burden could be also used in other malignancies such as breast carcinomas. Lastly, by enabling the examination of the entire tissue block using thin virtual recuts, microCT is the ultimate sampling method for the capsule of the tumor as well as the rest of the tissue. If this technique is one day popularized, the pathologists of the future will scroll through the CT images and be able to safely and surely finally state that they examined the entire tumor from all tumor blocks of their patients.

Supplementary Material

Refer to Web version on PubMed Central for supplementary material.

Acknowledgments

Research reported in this publication was supported in part by the Cancer Center Support Grant of the National Institutes of Health/National Cancer Institute under award number P30CA008748. The content is solely the responsibility of the authors and does not necessarily represent the official views of the National Institutes of Health.

REFERENCES

1. Rosai J, DeLellis RA, Carcangiu ML, Frable WJ, Tallini G. Tumor of the thyroid and parathyroid gland (AFIP atlas of tumor pathology series 4). American Registry of Pathology Press: Silver Spring, MD, 2015 606 pp.
2. Lloyd RV, Osamura RY, Kloppel G, Rosai J. WHO classification of tumours of endocrine organs. International Agency for Research on Cancer (IARC): Lyon, 2017.
3. Haugen BRM, Alexander EK, Bible KC, Doherty G, Mandel SJ, Nikiforov YE, et al. 2015 American Thyroid Association Management Guidelines for Adult Patients with Thyroid Nodules and Differentiated Thyroid Cancer. Thyroid 2016;26:1–133. [PubMed: 26462967]
4. Haddad RI, Lydiatt WM, Bischoff L, Busaidy NL, Byrd DR, Callender G, et al. NCCN clinical practive guidelines in oncology (NCCN guidelines): thyroid carcinoma. Version 1.2019. https://www.nccn.org/professionals/physician_gls/pdf/thyroid.pdf. 2019 Accessed: 7/15/2019.
5. Hanna MG, Reuter VE, Hameed MR, Tan LK, Chiang S, Sigel C, et al. Whole slide imaging equivalency and efficiency study: experience at a large academic center. Mod Pathol 2019;32:916–28. [PubMed: 30778169]
6. Boyce BF. An update on the validation of whole slide imaging systems following FDA approval of a system for a routine pathology diagnostic service in the United States. Biotech Histochem 2017;92:381–9. [PubMed: 28836859]
7. Farahani N, Braun A, Jutt D, Huffman T, Reder N, Liu Z, et al. Three-dimensional Imaging and Scanning: Current and Future Applications for Pathology. J Pathol Inform 2017;8:36. [PubMed: 28966836]
8. Senter-Zapata M, Patel K, Bautista PA, Griffin M, Michaelson J, Yagi Y. The Role of Micro-CT in 3D Histology Imaging. Pathobiology 2016;83:140–7. [PubMed: 27100885]
9. Sarraj WM, Tang R, Najjar AL, Griffin M, Bui AH, Zambeli-Ljepovic A, et al. Prediction of primary breast cancer size and T-stage using micro-computed tomography in lumpectomy specimens. J Pathol Inform 2015;6:60. [PubMed: 26730350]
10. Tang R, Coopey SB, Buckley JM, Aftreth OP, Fernandez LJ, Brachtel EF, et al. A pilot study evaluating shaved cavity margins with micro-computed tomography: a novel method for predicting lumpectomy margin status intraoperatively. Breast J 2013;19:485–9. [PubMed: 23773680]
11. Tang R, Saksena M, Coopey SB, Fernandez L, Buckley JM, Lei L, et al. Intraoperative micro-computed tomography (micro-CT): a novel method for determination of primary tumour dimensions in breast cancer specimens. Br J Radiol 2016;89:20150581. [PubMed: 26568439]
12. Nikiforov YE, Seethala RR, Tallini G, Baloch ZW, Basolo F, Thompson LD, et al. Nomenclature Revision for Encapsulated Follicular Variant of Papillary Thyroid Carcinoma: A Paradigm Shift to Reduce Overtreatment of Indolent Tumors. JAMA Oncol 2016;2:1023–9. [PubMed: 27078145]
13. Mete O, Seethala RR, Asa SL, Bullock MJ, Carty SE, Hodak SP, et al. College of American Pathologists: Protocol for the Examination of Specimens From Patients With Carcinomas of the Thyroid Gland. https://documents.cap.org/protocols/cp-endocrine-thyroid-19-4200.pdf. 2019 Accessed: 1/10/2020 2019.
14. Ghossein R, Barletta JA, Bullock MJ, Johnson SJ, Kakudo K, Lam A, et al. Dataset for the reporting of thyroid carcinoma from the International Collaboration on Cancer Reporting (ICCR). http://www.iccr-cancer.org/getattachment/Datasets/Published-Datasets/Endocrine-Organs/

Carcinoma-of-the-Thyroid-TNM8/ICCR-Thyroid-1st-edn-v1-0-bookmarked.pdf. 2019 Accessed: 7/30/2019.

15. Nikiforov YE, Paul Ohori N. Follicular carcinoma, In: Nikiforov YE, Biddinger PW, Thompson LDR, (eds). Diagnostic Pathology and Molecular Genetics of the Thyroid. Eds. Lippincott Williams and Wilkins: Philadelphia; 2010 p 143.
16. Chan J Tumours of the thyroid and parathyroid glands, In: Fletcher CDM, (ed). Diagnostic Histopathology of tumours. . Churchill Livingstone Elsevier: Philadelphia; 2007.
17. Mete O, Asa SL. Pathological definition and clinical significance of vascular invasion in thyroid carcinomas of follicular epithelial derivation. Mod Pathol 2011;24:1545–52. [PubMed: 21804527]
18. Vodovnik A. Capsular vascular proliferation associated with thyroid paraganglioma. Histopathology 2002;41:273.
19. Akdur NC, Donmez M, Gozel S, Ustun H, Hucumenoglu S. Intravascular papillary endothelial hyperplasia: histomorphological and immunohistochemical features. Diagn Pathol 2013;8:167. [PubMed: 24125024]
20. Jung CK, Little MP, Lubin JH, Brenner AV, Wells SA Jr., Sigurdson AJ, et al. The increase in thyroid cancer incidence during the last four decades is accompanied by a high frequency of BRAF mutations and a sharp increase in RAS mutations. J Clin Endocrinol Metab 2014;99:E276–85. [PubMed: 24248188]
21. Nikiforov YE, Baloch ZW, Hodak SP, Giordano TJ, Lloyd RV, Seethala RR, et al. Change in Diagnostic Criteria for Noninvasive Follicular Thyroid Neoplasm With Papillarylike Nuclear Features. JAMA Oncol 2018;4:1125–6. [PubMed: 29902314]
22. Lloyd RV, Asa SL, LiVolsi VA, Sadow PM, Tischler AS, Ghossein RA, et al. The evolving diagnosis of noninvasive follicular thyroid neoplasm with papillary-like nuclear features (NIFTP). Hum Pathol 2018;74:1–4. [PubMed: 29339178]
23. Randolph GW, Duh QY, Heller KS, LiVolsi VA, Mandel SJ, Steward DL, et al. The prognostic significance of nodal metastases from papillary thyroid carcinoma can be stratified based on the size and number of metastatic lymph nodes, as well as the presence of extranodal extension. Thyroid 2012;22:1144–52. [PubMed: 23083442]
24. Ricarte-Filho J, Ganly I, Rivera M, Katabi N, Fu W, Shaha A, et al. Papillary thyroid carcinomas with cervical lymph node metastases can be stratified into clinically relevant prognostic categories using oncogenic BRAF, the number of nodal metastases, and extra-nodal extension. Thyroid 2012;22:575–84. [PubMed: 22471242]

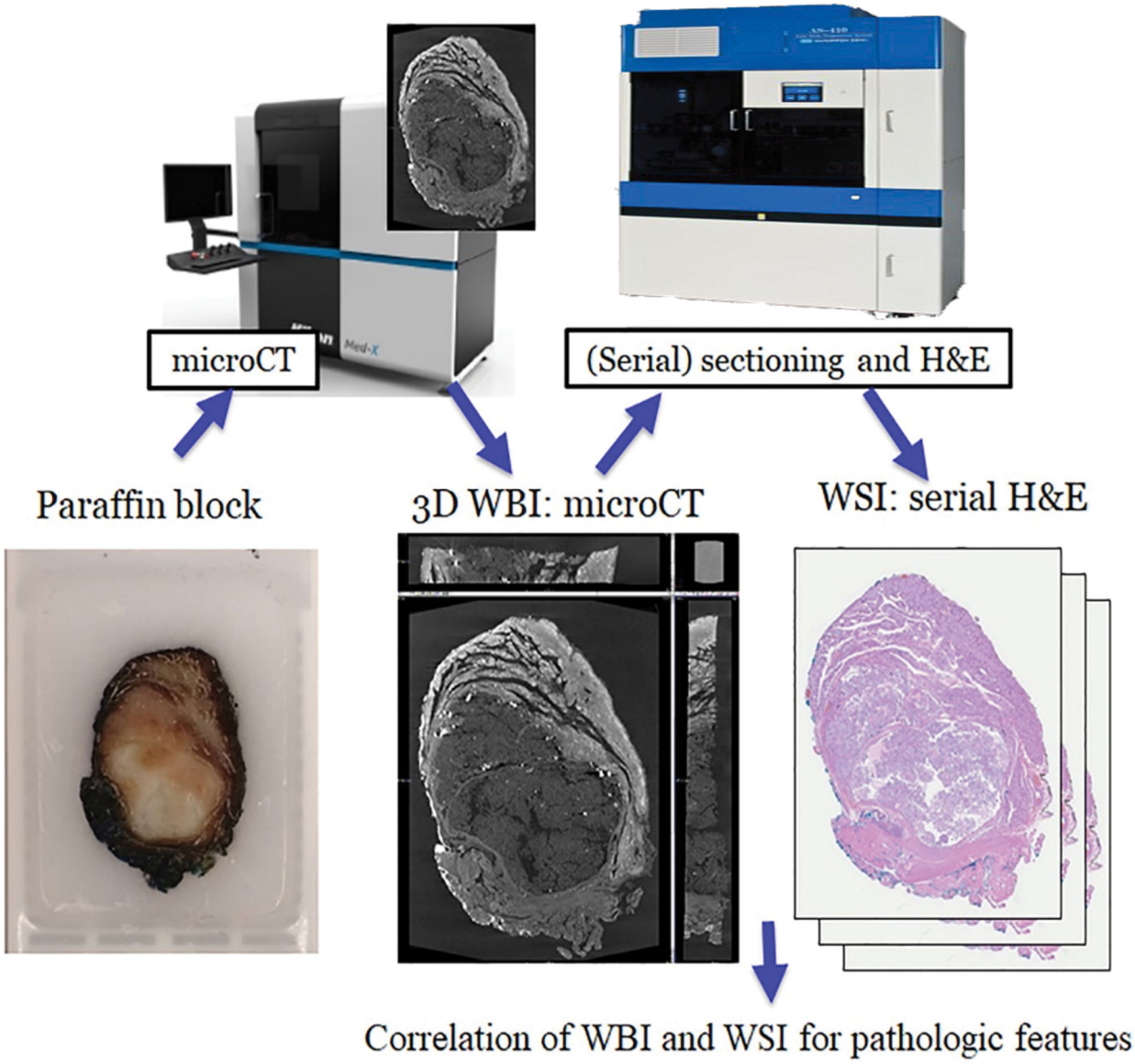

Figure 1. Diagram of the workflow.

Paraffin blocks are scanned with microCT to generate 3-dimensional microCT whole block images (WBI). Selected cases are subsequently serially sectioned and stained with hematoxylin and eosin (H&E) to generate whole slide images (WSI).

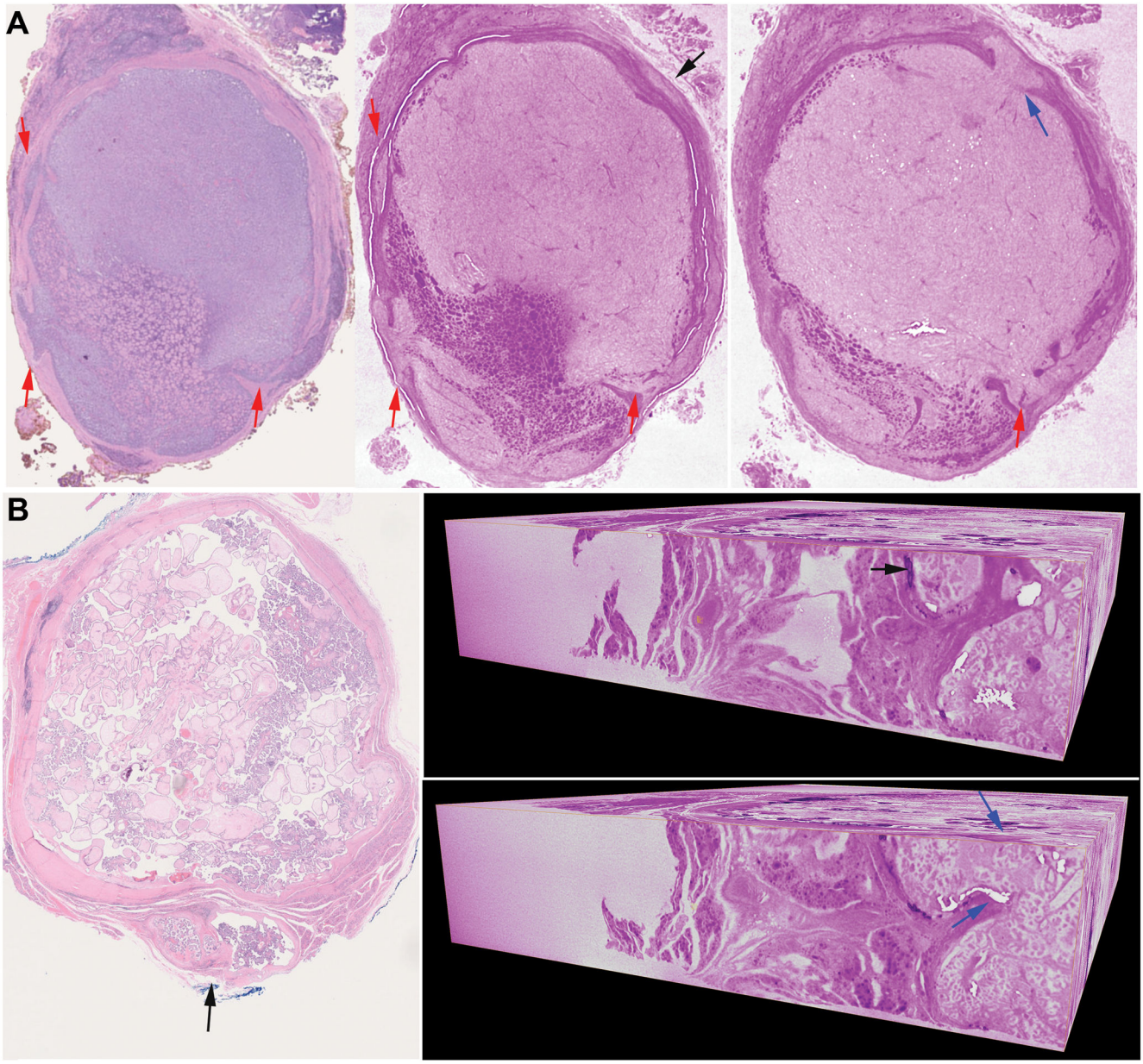

Figure 2. Capsular invasion (CI) demonstrated by using whole slide imaging (WSI) and whole block imaging (WBI) by microCT.

(A) A Hurthle cell carcinoma with multiple foci of CI. Left: WSI of the initial H&E shows 3 foci of CI (red arrows), Middle and right: microCT allows the detection of an additional focus of CI as a satellite nodule (middle, black arrow) on one virtual cut which ends up showing as a mushroom-shaped tumor bud with point of penetration (right, blue arrow) on a different cut. The micro CT images are digitally colored to give an H&E-like appearance. (B) A papillary thyroid carcinoma classic variant with one focus of CI (black arrow) on H&E slide (left). Right: 3D microCT images of the entire paraffin block showing a focus of CI as satellite nodule (black arrow) on one vertical virtual cut which ends up showing as

tumor bud penetrating the capsule (point of entry identified by blue arrows) on a different vertical cut.

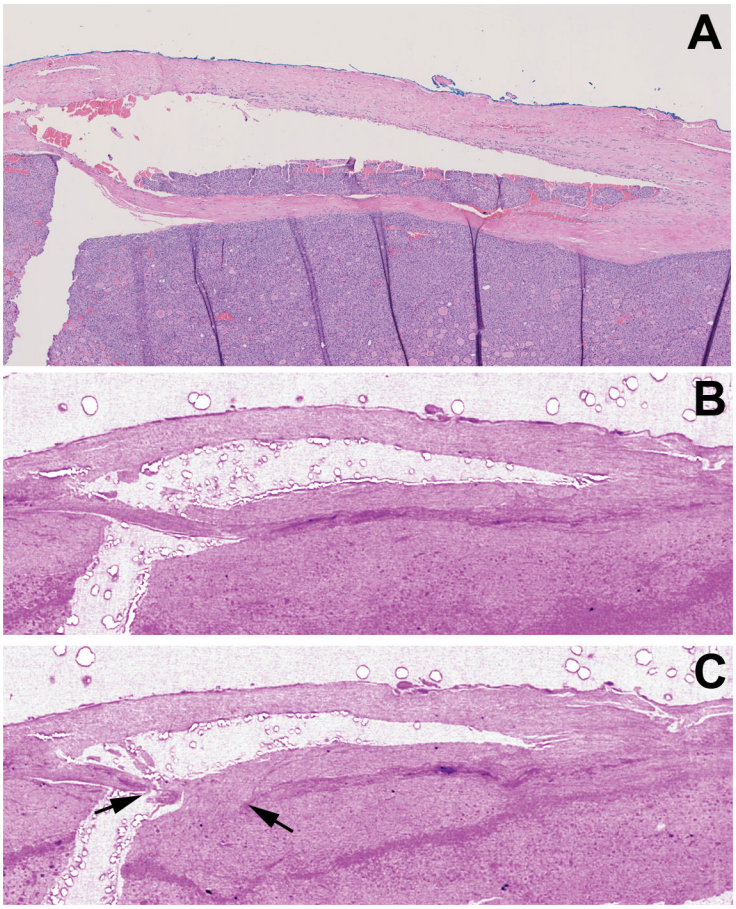

Figure 3. Vascular invasion (VI) detection using whole slide imaging (WSI) and whole block imaging (WBI) by microCT.

(A-C) Corresponding WSI of initial H&E (A) and serial microCT images (B-C) WBI may show VI and its point of entry (black arrows in C) on serial images. The micro CT images are digitally colored to give an H&E-like appearance.

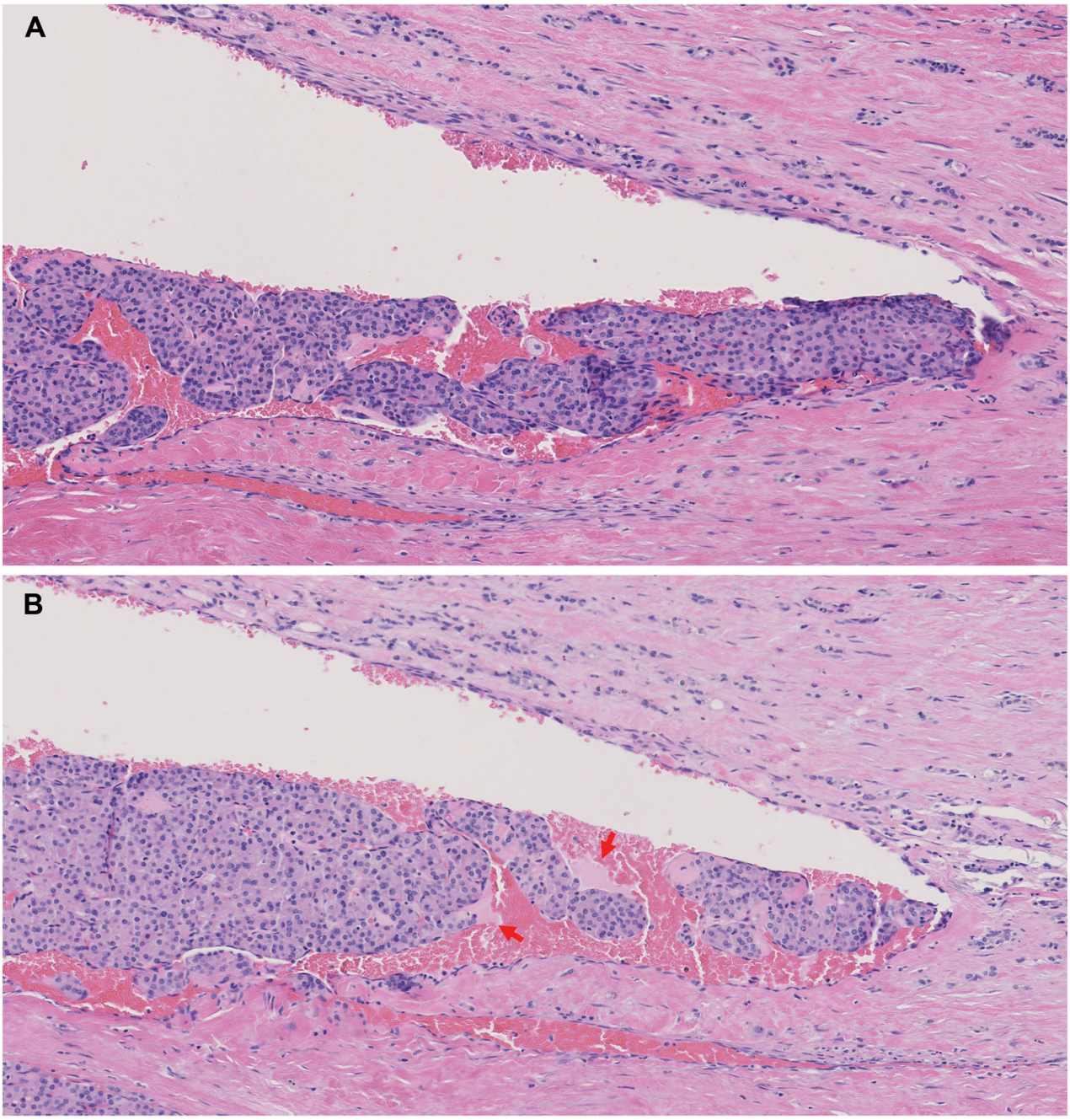

Figure 4. Vascular invasion (VI) associated with fibrin.

Serial sectioning and WSI of H&E stained sections from the same focus as in figure 2. WSI show that the fibrin (red arrows) is admixed with tumor thrombi in selected histologic levels (B) but not in all sections (A).

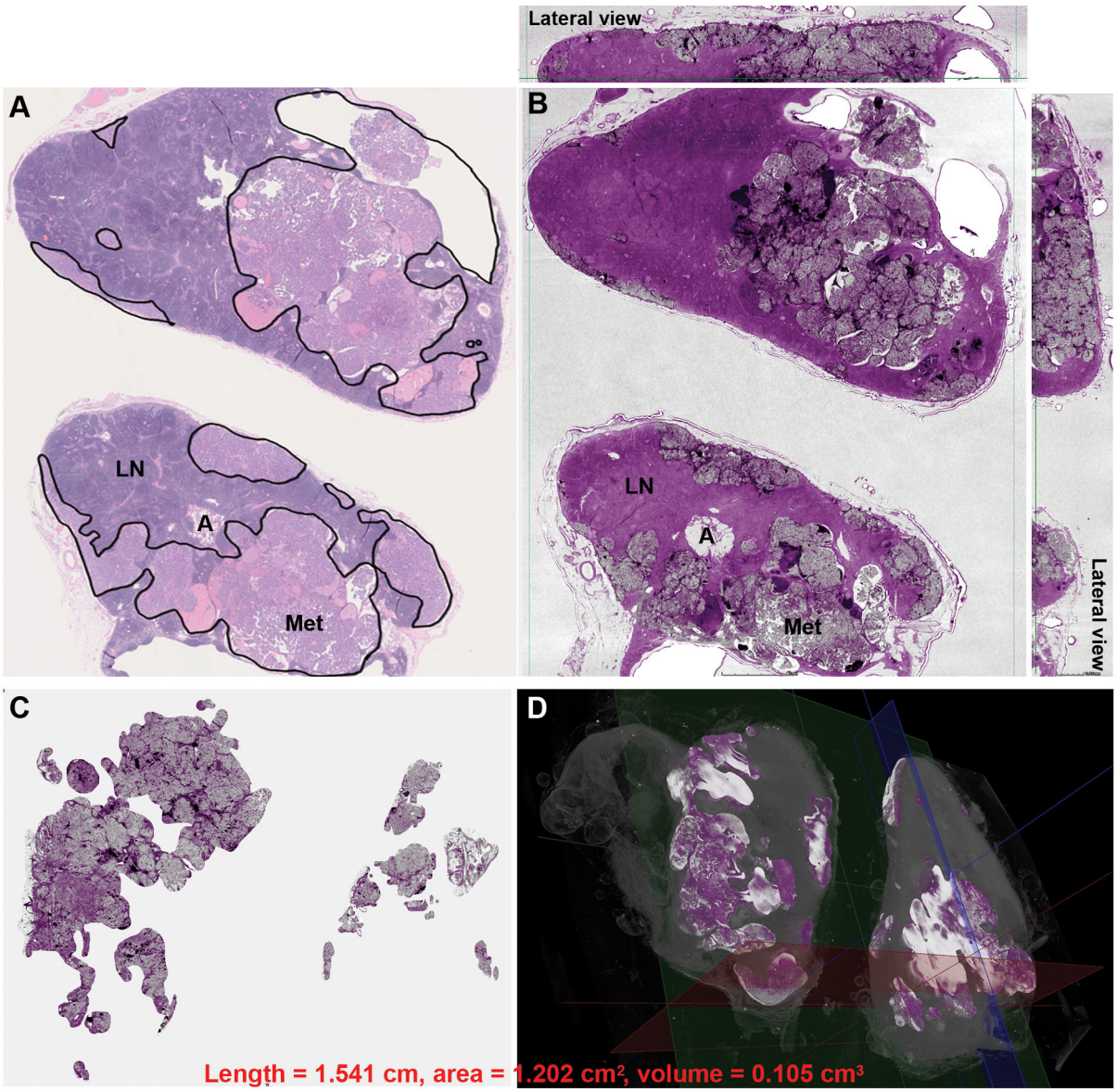

Figure 5. Assessment of metastatic papillary thyroid carcinoma burden in lymph nodes using whole slide imaging (WSI) (A) and whole block imaging (WBI) by microCT (B, C,D).

The area of metastasis is highlighted by black lines and the total surface area was calculated in WSI of H&E (A). Structures, e.g. uninvolved lymph node (LN), adipose tissue (A), and metastasis (Met), are readily identified in both WSI and WBI. The micro CT image in B is digitally colored to give an H&E-like appearance. The total volume of metastasis can be highlighted and calculated in 3D microCT images of WBI. (C) The background uninvolved lymph node is subtracted revealing only the metastatic focus. Note the irregular configuration of the metastatic focus in 3D. (D) The metastatic tumor volume highlighted in bright color in 3D.

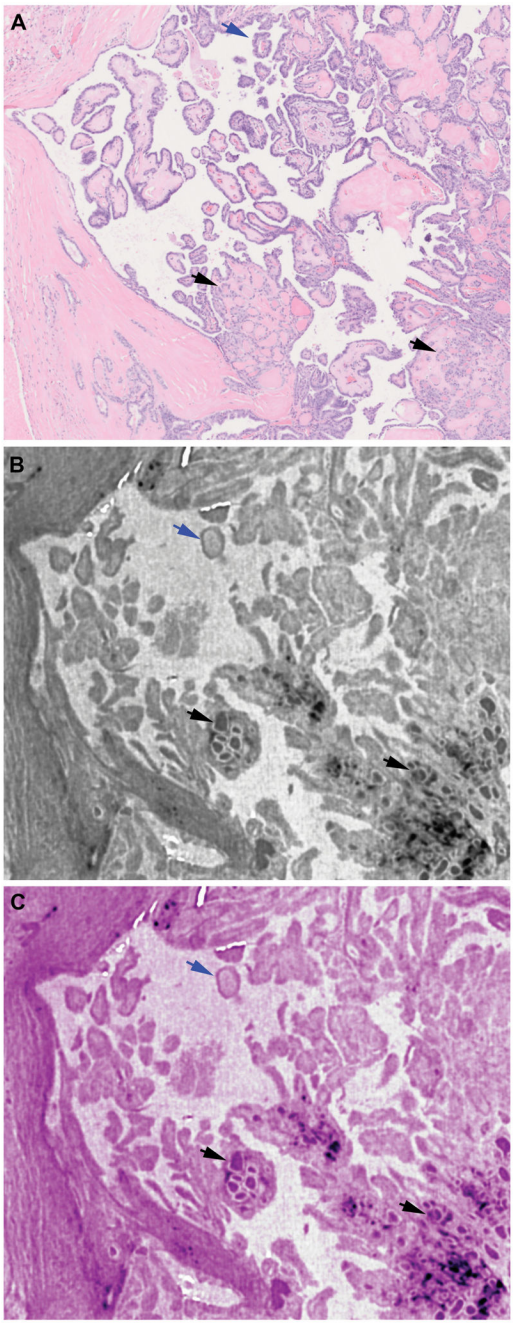

Figure 6. Visualization of papillae and follicles in a papillary thyroid carcinoma, classic using whole slide imaging (WSI) and whole block imaging (WBI) by microCT.

A: WSI of H&E slide with papillae (blue arrow) and follicles (black arrows). B and C: microCT images in greyscale (B) or digitally colored to give an H&E like appearance (C). Papillae (blue arrows) and follicles (black arrows) are easily identified by microCT.

Table 1.

Capsular invasion (CI) detected using whole slide imaging (WSI) and three-dimensional whole block imaging (WBI) by microCT.

Case Number	Diagnosis	CI in WSI		CI in WBI	
		Foci	Morphology	Foci	Morphology
1	PTC-CV	5	SN, POE	12	SN, POE
2	HCC	3	SN, POE	8	SN, POE
3	HCC	2	SN	2	SN
4	HCC	2	POE	2	POE
5	PTC-EFV	1	POE	1	SN
6	FTC	1	POE	1	POE
7	FTC	1	SN	1	SN
8	PTC-CV	1	POE	1	POE
9	PTC-CV	1	SN	1	POE
10	HCC	1	SN	1	POE
11	NIFTP	0	Incomplete penetration	0	Incomplete penetration

PTC-CV: papillary thyroid carcinoma, classic variant, HCC: Hurthle cell carcinoma, PTC-EFV: papillary thyroid carcinoma, encapsulated follicular variant, FTC: follicular thyroid carcinoma, NIFTP: noninvasive follicular thyroid neoplasm with papillary-like nuclear features, SN: satellite nodule, POE: point of entry (point of penetration).

Table 2.

Measurements of metastatic papillary thyroid carcinoma in lymph nodes using WSI and WBI.

	Length (mm)	Surface area (mm^2)	Volume (mm^3)
Lymph node 1	0.651	0.142	0.008
Lymph node 2	1.541	1.202	0.105
Fold difference between lymph nodes 2 and 1	2.367	8.465	13.125

Note: the surface area and volume calculation include metastatic foci of both halves of the bisected lymph node.